



The Effect of Linear, Parabolic and Inverted Parabolic Salinity Gradients on The Onset of Darcy Brinkman Rayleigh Benard Two-Component Convection in a Two-Layered System with Dufour Effect

Sumithra Ramakrishna¹, Shivaraja Munikrishnappa^{1,*}, Arul Selvamary Thomaiyar¹

¹ Department of Mathematics, Nrupathunga University, Karnataka, India

ARTICLE INFO

Article history:

Received 13 June 2022

Received in revised form 10 November 2022

Accepted 23 November 2022

Available online 14 December 2022

Keywords:

Dufour effect; two component convection; Rayleigh number; composite layer

ABSTRACT

The physical configuration of the problem of Darcy Brinkman (DB) Rayleigh Benard Two-Component (RBTC) Convection in a two-layered system has been investigated for linear, parabolic and inverted parabolic salinity gradients with the Dufour effect. For the fluid layer, the upper boundary is free with surface tension and for the porous layer, the lower boundary is rigid. At the interface, the normal velocity, normal stress, shear stress, mass, mass flux, heat, and heat flux are continuous. The regular perturbation method is used to solve the resulting ordinary differential equations obtained from normal mode expansion. The effect of different physical parameters on the Rayleigh number versus depth ratio is discussed and results are presented graphically.

1. Introduction

The Rayleigh Benard convection (RBC) is a type of natural convection, happening in a fluid layer, which placed horizontally and heated from underneath, wherein the layers fluid explores some common regular patterns corresponds to convective cells referred to as cells of Benard. RBC is one of the most typically studied convective phenomena due to its experimental as well as analytical accessibility. The problem we desire to analyse is one of Rayleigh-Benard (RB) Marangoni Convection in a system such as a porous layer underlying a fluid layer wherein there may be magnetic field through the device. The problem of fluid glide over a porous medium is encountered in an extensive variety of industrial and geophysical programs, along with flows in gas cells, filtration methods, the extraction of oil from underground reservoirs, and floor-water pollutants.

A detailed overview is given with the aid of Nield and Bejan [11] then Rana and Thakur [15] have explored the recent innovations in Double Diffusive (DD) convection in a viscoelastic fluid, which is placed in Darcy porous medium. For the porous medium, the Darcy Brinkman (DB) version is modelled moreover in Walters's analysis approach, the dispersion relation has been derived and

* Corresponding author.

E-mail address: shivarajajm95@gmail.com

<https://doi.org/10.37934/arfmts.101.2.121136>

solved analytically. It is found that the rotation, strong solute gradient, suspended debris, gravity field and viscoelasticity introduce oscillatory modes. The outcomes of rotation, stable solute gradient, suspended particles, Darcy number and medium permeability have also been investigated. Bhandaru and Vijaya [4] have been investigated heat and mass transfer by the impact of thermal conductivity and variable porosity regime in a rotating system. The governing equations for the boundary layer flow corresponding to species and energy are modified in the ODE system with the help of similarity transformation method and numerical methods (Shooting and Runge Kutta techniques) to solve the resulting system of ODEs. The impact of physical parameters thermal conductivity, concentration local skin friction and temperature are depicted graphically. Pal *et al.*, [13] have explored the recent innovations on Soret and Dufour effects along with the impact of variable thermal conductivity, magnetic field and ohmic dissipation. The numerical method (Runge-Kutta-Fehlberg) is used to solve the governing equations, they were concluding that enhance the Prandtl number then we observe the reduction in the micro rotation, velocity and temperature profiles and also species distribution is increased by decreasing or increasing the Dufour-Soret parameter. The numerical study of the self-diffusion of nanoparticles is very limited, Tan *et al.*, [7] demonstrated that the DPD method can be used to predict the diffusivity of nanoparticles. A good agreement between 3% and 30% can be obtained by comparing both previous experimental results and the Einstein correlation. Apart from that, the DPD method also managed to correctly simulate the Brownian motion of nanoparticles suspended in the base liquid. It is also worth noting that higher numbers of nanoparticles generally decrease diffusivity. Upcoming work will be done with more test cases with different parameters to improve the accuracy of the simulation. Altawallbeh [1] has considered a viscoelastic fluid to analyze the combining effect of diffusion thermal, thermal diffusion and internal heat source. On a saturated porous layer, Old Royd-type modified Darcy law is modelled for the momentum equation. The effect of internal heat, Soret, Dufour, relaxation and Rayleigh number on stationary and oscillatory convections are represented graphically and also mass transfer and heat are also depicted graphically in terms of Sherwood and Nusselt numbers respectively. Moreover, he discussed both linear and nonlinear stability. The role of the finite element method to find the solution of Darcy Brinkman Forchheimer's (DBF) equation of irregular flow has been investigated by Murali *et al.*, [9] the solution of nonlinear PDEs is obtained from the finite element approach (Gauss seidel and quasi linearization method) and the corresponding method is equipped with the help of some programming packages moreover they get the 10^{-5} accuracy in the final solution. The onset of Darcy-Rayleigh convection in a viscoelastic, doubly diffusive, binary fluid layer saturated in an anisotropic porous material with temperature-dependent viscosity is analyzed numerically. Abidin *et al.*, [12] has discussed the Rayleigh number from the doubly diffusive binary fluid was obtained using the Galerkin expansion method. The impacts of strain lag and thermal anisotropy parameters slow heat transfer formation as their values increase and stabilize the system. Meanwhile, the stress relaxation, Darcy-Prandtl, and mechanical anisotropy parameters rapidly enhanced the heat transfer mechanism in convection as the values increased, thereby destabilizing the system.

2. Mathematical Formulation

The physical model under the consideration of a composite layer system with a horizontal two-component fluid-saturated, incompressible, isotropic and sparsely packed porous layer is of thickness d_m and a fluid layer of thickness d . Both the boundaries of the composite layer system are considered to be rigid and these boundaries are acts like heat and mass insulators along with maintained, distinct concentration and temperature. The origin point of the Cartesian coordinate system is taken exactly

at the intersection of porous and fluid layer along with the direction of z – axis vertically upwards as shown in Figure 1.

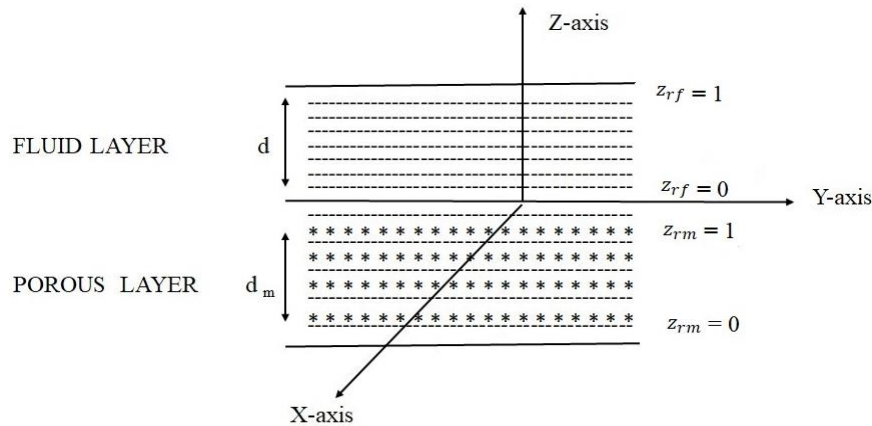


Fig. 1. Physical model of composite layer/two-layer system

The governing equations are, the continuity, momentum, temperature, concentration and state equations as follows.

For Region – 1 (fluid layer)

$$\nabla \cdot \vec{q}_{rf} = 0 \tag{1}$$

$$\rho_{0f} \left[\frac{\partial \vec{q}_{rf}}{\partial t} + (\vec{q}_{rf} \cdot \nabla) \vec{q}_{rf} \right] = -\nabla P_{rf} + \mu \nabla^2 \vec{q}_{rf} - \rho_{rf} g_{rf} \hat{k} \tag{2}$$

$$\frac{\partial T_{rf}}{\partial t} + (\vec{q}_{rf} \cdot \nabla) T_{rf} = \kappa_{rf} \nabla^2 T_{rf} + \kappa_{Trf} \nabla^2 C_{rf} \tag{3}$$

$$\frac{\partial C_{rf}}{\partial t} + (\vec{q}_{rf} \cdot \nabla) C_{rf} = \kappa_{rsf} \nabla^2 C_{rf} \tag{4}$$

$$\rho_{rf} = \rho_{0f} [1 + \alpha_{rf}(C_{rf} - C_{0f}) - \alpha_{2f}(T_{rf} - T_{0f})] \tag{5}$$

For Region – 2 (porous layer)

$$\nabla_{rm} \cdot \vec{q}_{rm} = 0 \tag{6}$$

$$\left[\frac{\rho_{0f}}{\phi_m} \right] \frac{\partial \vec{q}_{rm}}{\partial t_{rm}} = -\nabla_{rm} p_{rm} - \frac{\mu}{\kappa_{rm}} \vec{q}_{rm} + \mu_{rm} \nabla_{rm}^2 \vec{q}_{rm} - \rho_{rm} g_{rf} \hat{k} \tag{7}$$

$$A \left[\frac{\partial T_{rm}}{\partial t_{rm}} \right] + (\vec{q}_{rm} \cdot \nabla_{rm}) T_{rm} = \kappa_{rm} \nabla_{rm}^2 T_{rm} + \kappa_{rmT} \nabla_{rm}^2 C_{rm} \tag{8}$$

$$\phi \left[\frac{\partial C_{rm}}{\partial t_{rm}} \right] + (\vec{q}_{rm} \cdot \nabla_{rm}) C_{rm} = \kappa_{rsm} \nabla_{rm}^2 C_{rm} \tag{9}$$

$$\rho_{rm} = \rho_{0f} [1 - \alpha_{rm}(T_{rm} - T_{0f}) + \alpha_{2m}(C_{rm} - C_{0f})] \tag{10}$$

where,

$\vec{q}_{rf}, t, \mu, P_{rf}, \rho_{rf}, g_{rf}, T_{rf}, \kappa_{rf}, \kappa_{rsf}, \kappa_{Tf}, C_{rf}, \phi_m, K_{rm}, \mu_{rm}, \alpha_{rf}, \alpha_{rm}, A = \frac{(\rho_{of} c_p)_m}{(\rho_{rf} c_p)_f}, C_p, \rho_{of}$ are the fluid layer velocity vector, time, viscosity of fluid, pressure, density of fluid, gravity, temperature, thermal diffusivity, solutal diffusivity, Dufour coefficient, concentration, thermal expansion coefficient, a solutal analog of α_{2f} , porosity of the porous medium, permeability of the porous medium, porous medium effective viscosity, heat capacities ratio, specific heat and referring fluid respectively. In the porous medium, the quantities are referred to by the subscripts m .

Basic/Primary state conditions are implemented to the governing equations which are in the form of partial differential equations (PDEs) to discover the answers to the basic state. The set-up is taken into consideration by undergoing super-imposition with infinitely small perturbations. The equations are then linearized using the units of perturbations after that resulting equations are going to be non-dimensionalised with the help of non-dimensional variables and normalized which turns PDEs are reduced to a system of ODEs [11].

For Region - 1 (fluid layer)

$$D_{rf}^2 - a_{rf}^2W_{rf} = R_{rf} a_{rf}^2 \theta_{rf} - R_{srf} a_{rf}^2 S_{rf} \quad (11)$$

$$(D_{rf}^2 - a_{rf}^2)\theta + W_{rf} + D_R(D_{rf}^2 - a_{rf}^2) S_{rf} = 0 \quad (12)$$

$$[\tau(D_{rf}^2 - a_{rf}^2)] S_{rf} + W_{rf} = 0 \quad (13)$$

For region - 2 (porous layer)

$$[\widehat{\mu} \beta^2 (D_{rm}^2 - a_{rm}^2) - 1](D_{rm}^2 - a_{rm}^2)W_{rm} = R_{rm} a_{rm}^2 \theta_{rm} - R_{srm} a_{rm}^2 S_{rm} \quad (14)$$

$$(D_{rm}^2 - a_{rm}^2)\theta_{rm} + W_{rm} + D_{MR}(D_{rm}^2 - a_{rm}^2)S_{rm} = 0 \quad (15)$$

$$[\tau_{pm}(D_{rm}^2 - a_{rm}^2)] S_{rm} + W_{rm} = 0 \quad (16)$$

where, for the fluid layer, $D_{rf} = \frac{d_{rf}}{dz_{rf}}$ is the differential operator with respect to z_{rf} ,

$p_r = \frac{\nu}{k_{rf}}$ is the Prandtl number,

$\tau = \frac{k_{rf}}{k_{rsf}}$ is the ratio of thermal diffusivity to solute diffusivity,

$\nu = \frac{\mu}{\rho_{of}}$ is the kinematic viscosity,

$R_{rf} = \frac{g \alpha_{rf} (T_{of} - T_{rf}) d^3}{\nu k_{rf}}$ is the Rayleigh number,

$R_{Srf} = \frac{g \alpha_{2f}(C_{0f}-C_{rf}) d^3}{\nu k_{rf}}$ is the solute Rayleigh number and

$D_R = \frac{k_{Trf}(C_{0f}-C_{rf})}{k_{rf}(T_{0f}-T_{rf})}$ is Dufour coefficient.

For the porous layer, $D_{rm} = \frac{d_{rm}}{dz_{rm}}$ is the differential operator with respect to z_{rm} ,

$p_{rm} = \frac{\phi \nu}{k_{rm}}$ is the Prandtl number,

$\beta^2 = \frac{K_{rm}}{d_m^2} = D_a$ is the Darcy number,

$\tau_{pm} = \frac{k_{rm}}{k_{rsm}}$ is the ratio of thermal diffusivity to solute diffusivity,

$D_{MR} = \frac{k_{rmT}(C_{rm}-C_{0f})}{k_{rm}(T_{rm}-T_{0f})}$ is the Dufour coefficient,

$R_{rm} = \frac{g \alpha_{rf}(T_{rm}-T_{0f}) d^3}{\nu k_{rm}}$ is the Rayleigh number,

$R_{Srm} = \frac{g \alpha_{2m}(C_{rm}-C_{0f}) d^3}{\nu k_{rm}}$ is the solute Rayleigh number and $\hat{\mu} = \frac{\mu_{rm}}{\mu}$ is the viscosity ratio.

3. Boundary Conditions

The appropriate non-dimensionalized and normalized boundary conditions for both upper and lower boundaries, at interfaces, are mentioned below.

$$W_{rf}(1) = 0, D_{rf}W_{rf}(1) = 0, D_{rf}\Theta_{rf}(1) = 0, D_{rf}S_{rf}(1) = 0$$

$$\hat{T}W_{rf}(0) = W_{rm}(1), \hat{T}\hat{d}D_{rf}W_{rf}(0) = D_{rm}W_{rm}(1), \Theta_{rf}(0) = \hat{T}\Theta_{rm}(1),$$

$$D_{rf}\Theta_{rf}(0) = D_{rm}\Theta_{rm}(1), S_{rf}(0) = \hat{S}S_{rm}(1), D_{rf}S_{rf}(0) = D_{rm}S_{rm}(1)$$

$$\hat{T}d^3\beta^2[D_{rf}^3W_{rf}(0) - 3a^2D_{rf}W_{rf}(0)] = \left\{ \begin{array}{l} -D_{rm}W_{rm}(1) \\ + \hat{\mu}\beta^2\beta^2[D_{rm}^3W_{rm}(1) - 3a_{rm}^2D_{rm}W_{rm}(1)] \end{array} \right\}$$

$$\hat{T}\hat{d}^2[(D_{rf}^2 + a^2)W_{rf}(0)] = \hat{\mu}(D_{rm}^2 + a_{rm}^2)W_{rm}(1)$$

$$W_{rm}(0) = 0, D_{rm}W_{rm}(0) = 0, D_{rm}\Theta_{rm}(0) = 0, D_{rm}S_{rm}(0) = 0$$

where,

$$\hat{d} = \frac{d_m}{d}, \hat{k} = \frac{\hat{d}}{\hat{T}} = \frac{k_{rm}}{k_{rf}}, \hat{k}_s = \frac{k_{rsm}}{k_{rsf}} = \frac{\hat{d}}{\hat{S}}, \hat{T} = \left[\frac{T_{rm} - T_{0f}}{T_{0f} - T_{rf}} \right], \hat{S} = \left[\frac{C_{rm} - C_{0f}}{C_{0f} - C_{rf}} \right]$$

4. Regular Perturbation Technique

For the consistent mass and heat fluxes, expanding the physical parameters in terms of horizontal wave numbers " a_{rf} " and " a_{rm} "

$$\begin{bmatrix} W_{rf} \\ \Theta_{rf} \\ S_{rf} \end{bmatrix} = \sum_{i=0}^{\infty} a_{rf}^{2i} \begin{bmatrix} W_{rfi} \\ \Theta_{rfi} \\ S_{rfi} \end{bmatrix} \quad \& \quad \begin{bmatrix} W_{rm} \\ \Theta_{rm} \\ S_{rm} \end{bmatrix} = \sum_{i=0}^{\infty} a_{rm}^{2i} \begin{bmatrix} W_{rmi} \\ \Theta_{rmi} \\ S_{rmi} \end{bmatrix}$$

To find the Solution of zero order equations using the arbitrary factors as mentioned below

$$W_{rf0}(z_{rf}) = 0, W_{rm0}(z_{rm}) = 0, S_{rf0}(z_{rf}) = \hat{S}, S_{rm0}(z_{rm}) = 1, \Theta_{rf0}(z_{rf}) = \hat{T}, \Theta_{rm0}(z_{rm}) = 1$$

First-order equations For the Fluid layer ($z_{rf} \in [0,1]$) are mentioned below

$$D_{rf}^4 W_{rf1} - R_{rf} \hat{T} + R_{srf} \hat{S} = 0 \tag{17}$$

$$D_{rf}^2 \Theta_{rf1} + W_{rf1} + D_R(D_{rf}^2 S_{rf1} - \hat{S}) - \hat{T} = 0 \tag{18}$$

$$\tau D_{rf}^2 S_{rf1} + W_{rf1} - \tau \hat{S} = 0 \tag{19}$$

First-order equations for the porous layer ($z_{rm} \in [0,1]$) are mentioned below

$$\hat{\mu} \beta^2 D_{rm}^4 W_{rm1} - D_{rm}^2 W_{rm1} - R_{rm} + R_{srm} = 0 \tag{20}$$

$$D_{rm}^2 \Theta_{rm1} + W_{rm1} + D_{MR} D_{rm}^2 S_{rm1} - D_{MR} - 1 = 0 \tag{21}$$

$$\tau_m D_{rm}^2 S_{rm1} + W_{rm1} - \tau_m = 0 \tag{22}$$

Boundary conditions related to 1st order equations are given below.

$$W_{rf1}(1) = 0, D_{rf1} W_{rf1}(1) = 0, D_{rf1} \Theta_{rf1}(1) = 0, D_{rf1} S_{rf1}(1) = 0$$

$$\hat{T} W_{rf1}(1) = \hat{d}^2 W_{rm1}(0), \hat{T} D_{rf1} W_{rf1}(1) = \hat{d} D_{rm1} W_{rm1}(0), \Theta_{rf1}(1) = \hat{d}^2 \hat{T} \Theta_{rm1}(0)$$

$$D_{rf1} \Theta_{rf1}(1) = \hat{d}^2 D_{rm1} \Theta_{rm1}(0), S_{rf1}(1) = \hat{S} \hat{d}^2 S_{rm1}(0), D_{rf1} S_{rf1}(1) = D_{rm1} S_{rm1}(0)$$

$$\hat{T} \hat{d} \beta^2 D_{rf1}^3 W_{rf1}(1) = -D_{rm1} W_{rm1}(0) + \hat{\mu} \beta^2 [D_{rm1}^3 W_{rm1}(0)], D_{rm1} S_{rm1}(0) = 0$$

$$\hat{T} D_{rf1}^2 W_{rf1}(1) = \hat{\mu} D_{rm1}^2 W_{rm1}(0), W_{rm1}(0) = 0, D_{rm1} W_{rm1}(0) = 0, D_{rm1} \Theta_{rm1}(0) = 0$$

Eq. (17) and Eq. (20) are solved using the relevant boundary conditions then we get velocity distributions as below,

$$W_{rf1}(z_{rf}) = \left[\frac{\hat{T} R_{rf} - \hat{S} R_{srf}}{24} \right] (C_1 + C_2 z_{rf} + C_3 z_{rf}^2 + C_4 z_{rf}^3 + z_{rf}^4) \tag{23}$$

$$W_{rm1}(z_{rm}) = C5 + C6z_{rm} + C7e^{pz_{rm}} + C8e^{-pz_{rm}} + \mathcal{M} \quad (24)$$

$$\mathcal{M} = \frac{(R_{srm}-R_{rm})z_{rm}^2}{2} + \frac{(R_{srm}-R_{rm})}{p^2} \quad (25)$$

5. Compatibility Condition

The differential equations corresponding to concentration and temperature, along with corresponding boundary conditions give the compatibility condition as below.

$$\left\{ \begin{array}{l} \int_0^1 W_{rf1}(z_{rf}) dz_{rf} - \frac{D_R}{\tau} \int_0^1 W_{rf1}(z_{rf}) f(z_{rf}) dz_{rf} \\ + \widehat{d}^2 \int_0^1 W_{rm1}(z_{rm}) dz_{rm} - \frac{D_{MR}}{\tau_m} \widehat{d}^2 \int_0^1 W_{rm1}(z_{rm}) g(z_{rm}) dz_{rm} \end{array} \right\} = \widehat{d}^2 + \widehat{T} \quad (26)$$

In the above expression, $f(z_{rf})$ and $g(z_{rm})$ are taken according to basic salinity gradients.

5.1 Linear Salinity Profile (LSP)

The Rayleigh number is obtained by substituting $f(z_{rf}) = 1$ and $g(z_{rm}) = 1$ in Eq. (26).

$$\mathbb{R}_L = \left\{ \left[\frac{\widehat{d}^2}{\widehat{T}(\mathcal{M}_1 - \hbar_1 \mathcal{M}_2)} \right] + \left[\frac{R_{srm} \widehat{C}(\mathcal{M}_1 - \hbar_1 \mathcal{M}_2)}{\widehat{T}(\mathcal{M}_1 - \hbar_1 \mathcal{M}_2)} \right] + \left[\frac{1}{(\mathcal{M}_1 - \hbar_1 \mathcal{M}_2)} \right] \right\}$$

where,

$$\mathbb{C} = e^{-\vartheta}; l = e^{\vartheta}; \mathbb{C}_1 = (\beta^2 \widehat{d})^{-1} \beta = (Da)^{1/2}; \vartheta = (\mu \beta^2)^{-1/2}; \theta_3 = 12\mu\mathbb{C} - 4\mathbb{C}\mathbb{C}_1$$

$$F_3 = 24\widehat{d}\mathbb{C} + 24\mu\mathbb{C} - 12\mathbb{C}\mathbb{C}_1; F_2 = 24\widehat{d}\mathbb{C}\vartheta(1 - \mathbb{C}) + 24\vartheta^2\mu\mathbb{C}^2 + \theta_1; \hbar_5 = \mathring{A}_1(N_3F_2 - N_2F_3);$$

$$\theta_1 = 12\vartheta\mathbb{C}^2(1 - \vartheta - l)\mathbb{C}_1; F_1 = 24\widehat{d}\vartheta(1 - \mathbb{C}) + 24\vartheta^2\mu + \theta_2; \hbar_4 = \mathring{A}_2 \widehat{T}\mathbb{C}(4N_1 - F_1);$$

$$\theta_2 = 12\vartheta(\mathbb{C} + \vartheta - 1)\mathbb{C}_1; N_3 = 12\widehat{d}^2\mathbb{C} + 24\mathbb{C}\widehat{d} + \theta_3; N_2 = 24\widehat{d}^2(\vartheta - 1 + \mathbb{C})\mathbb{C} + 24\widehat{d}\vartheta\mathbb{C} + \theta_4;$$

$$\theta_4 = 12\vartheta^2\mu\mathbb{C}^2 + 4\mathbb{C}^2\vartheta(1 - \vartheta - l)\mathbb{C}_1; N_1 = 24\widehat{d}^2(-\mathbb{C}\vartheta + 1 - \mathbb{C}) + 12\mu\mathbb{C}^2 + \theta_5;$$

$$\theta_5 = 24\widehat{d}\vartheta(1 - \mathbb{C}) + 4\vartheta(\vartheta - 1 + \mathbb{C})\mathbb{C}_1; \hbar_6 = \mathring{A}_2(N_1F_3 - N_3F_1); \hbar_2 = N_2F_2 - N_3F_2;$$

$$\hbar_1 = \frac{\widehat{\beta}^2 \widehat{d}^3}{\widehat{k}}; \mathcal{M}_1 = \frac{\hbar_3}{\hbar_2} + \frac{\hbar_4}{\hbar_2} + \frac{\tau - D_R}{120}; \mathcal{M}_2 = \mathring{A}_3 + \frac{\hbar_5}{\hbar_2} + \frac{\hbar_6}{\hbar_2}; \hbar_3 = \mathring{A}_1 \widehat{T} * \mathbb{C}(F_2 - 4N_2)$$

$$\hbar_7 = \frac{\tau - D_R}{24 \tau \widehat{T} \widehat{d} \beta^2}; \mathring{A}_3 = \hbar_7 + \hbar_9 + \frac{\hbar_{11}}{2} + \frac{\hbar_{11}\widehat{d}}{2} + \frac{1}{6}; \hbar_{11} = \frac{(\tau - D_R)\widehat{d}}{\tau \widehat{T}}; \hbar_{12} = \frac{\vartheta(1 - \mathbb{C})}{2\mathbb{C}};$$

$$\mathring{A}_1 = \hbar_7 \hbar_8 + \hbar_9 \hbar_{10} + \hbar_{11} \hbar_{12} + \hbar_{11} \hbar_{13} - \hbar_{14} - \hbar_{15} + \hbar_{16}(\mathbb{C} - 1); \hbar_{19} = \frac{\vartheta(1 - \mathbb{C})}{2};$$

$$\mathring{A}_2 = \mathring{h}_7 \mathring{h}_{17} + \mathring{h}_9 \mathring{h}_{18} + \mathring{h}_{11} \mathring{h}_{19} + \mathring{h}_{11} \mathring{h}_{20} - \mathring{h}_{14} + \mathring{h}_{15} + \mathring{h}_{16} \mathbb{C} - \mathring{h}_{16}; \mathring{h}_{20} = \hat{d}(\mathcal{G} + \mathbb{C}) - \hat{d};$$

$$\mathring{h}_{13} = \frac{(1 - \mathcal{G}\mathbb{C} - \mathbb{C})\hat{d}}{\mathbb{C}}; \mathring{h}_{14} = \frac{\tau_m \hat{d}^2 - D_{MR} \hat{d}^2}{\tau_m}; \mathring{h}_{18} = \mathcal{G}^2 \mathbb{C}; \mathring{h}_{10} = \frac{\mathcal{G}^2}{\mathbb{C}}; \mathring{h}_8 = \mathcal{G}(\mathcal{G} - 1 + \mathbb{C})l$$

$$\mathring{h}_{15} = \frac{\mathcal{G}(\tau_m \hat{d}^2 - D_{MR} \hat{d}^2)}{2\tau_m}; \mathring{h}_{16} = \frac{(\tau_m \hat{d}^2 - D_{MR} \hat{d}^2)}{\mathcal{G}\tau_m}; \mathring{h}_{17} = \mathcal{G}(1 - \mathcal{G} - l)\mathbb{C};$$

5.2 Parabolic Salinity Profile (PSP)

The Rayleigh number is obtained by substituting $f(z_{rf}) = 2 z_{rf}$ and $g(z_{rm}) = 2 z_{rm}$ in Eq. (26).

$$\mathbb{R}_L = \left\{ \left[\frac{\hat{d}^2}{\hat{T}(\mathcal{M}_1 - \mathring{h}_1 \mathcal{M}_2)} \right] + \left[\frac{R_{srm} \hat{C} (\mathcal{M}_1 - \mathring{h}_1 \mathcal{M}_2)}{\hat{T}(\mathcal{M}_1 - \mathring{h}_1 \mathcal{M}_2)} \right] + \left[\frac{1}{(\mathcal{M}_1 - \mathring{h}_1 \mathcal{M}_2)} \right] \right\}$$

where,

$$\mathring{h}_1 = \frac{\widehat{\beta^2 d^3}}{\hat{k}}; \mathcal{M}_1 = \frac{\mathring{h}_3}{\mathring{h}_2} + \frac{\mathring{h}_4}{\mathring{h}_2} + \frac{3\tau\tau_m - 3D_R\tau_m}{360};$$

$$\mathcal{M}_2 = \mathring{A}_3 + \frac{\mathring{h}_5}{\mathring{h}_2} + \frac{\mathring{h}_6}{\mathring{h}_2}; \mathring{h}_7 = \frac{\mathcal{G}(\mathbb{C} + \mathcal{G} - 1)}{\mathbb{C}};$$

$$\mathring{A}_3 = \mathring{h}_{10} - \mathring{h}_8 + \mathring{h}_{12} + \mathring{h}_{22} + \frac{\tau \hat{d}^2 \tau_m}{6} + \frac{\tau \hat{d}^2 D_{MR}}{4};$$

$$\mathring{h}_8 = \left(\frac{\tau\tau_m}{4} - \frac{2D_R\tau_m}{5} \right) (6\tau\widehat{\beta^2 d})^{-1}; \mathring{h}_9 = \mathcal{G}^2 \mathbb{C};$$

$$\mathring{A}_1 = \mathring{h}_7 \mathring{h}_8 + \mathring{h}_9 \mathring{h}_{10} + \mathring{h}_{11} \mathring{h}_{12} + \mathring{h}_{13} + \mathring{h}_{14} - 2\mathring{h}_{15} \tau \hat{d}^2 D_{MR};$$

$$\mathring{A}_2 = \mathring{h}_8 \mathring{h}_{16} + \mathring{h}_{10} \mathring{h}_{17} + \mathring{h}_{12} \mathring{h}_{18} + \mathring{h}_{19} + \mathring{h}_{20} - 2\mathring{h}_{15} \tau \hat{d}^2 D_{MR};$$

$$\mathring{h}_{11} = \mathcal{G}(1 - \mathbb{C})l; \mathring{h}_{12} = \left(\frac{\tau\tau_m}{2} - \frac{2D_R\tau_m}{3} \right) \left(\frac{\hat{d}}{\hat{T}} \right); \mathring{h}_{18} = \mathcal{G}(1 - \mathbb{C});$$

$$\mathring{h}_{13} = \frac{\hat{d}^2(1 - \mathcal{G}\mathbb{C} - \mathbb{C})(\tau\tau_m - D_R\tau_m)}{\hat{T} \mathbb{C}}; \mathring{h}_{16} = \mathcal{G} \mathbb{C}(1 - \mathcal{G} - l);$$

$$\mathring{h}_{19} = \frac{\hat{d}^2(-1 + \mathcal{G} + \mathbb{C})(\tau\tau_m - D_R\tau_m)}{\hat{T}}; \mathring{h}_{22} = \frac{\hat{d}^2(\tau\tau_m - D_R\tau_m)}{\hat{T}};$$

$$\mathring{h}_{20} = \tau\tau_m \hat{d}^2 \left(-1 + \frac{\mathcal{G}}{2} - \frac{\mathbb{C} - 1}{\mathcal{G}} \right); \mathring{h}_{21} = \frac{2\mathcal{G} - 3}{6} + \frac{1 - \mathbb{C} - \mathcal{G} \mathbb{C}}{\mathcal{G}^2};$$

$$\begin{aligned} \hbar_{10} &= \left(\frac{\tau\tau_m}{3} - \frac{D_R\tau_m}{2} \right) \left(\frac{\mu}{2\hat{T}} \right); \hbar_{14} = \tau\tau_m \hat{d}^2 \left(-1 - \frac{\mathcal{G}}{2} + \frac{l-1}{\mathcal{G}} \right); \\ \hbar_{15} &= \frac{-3-2\mathcal{G}}{6} + \frac{\mathcal{G}l-l+1}{\mathcal{G}^2}; \hbar_{17} = \mathcal{G}^2 \mathbb{C}; \hbar_{18} = \mathcal{G}(1-\mathbb{C}); \end{aligned}$$

5.3 Inverted parabolic Salinity Profile (ISP)

The Rayleigh number is obtained by substituting $f(z_{rf}) = 2(1 - z_{rf})$ and $g(z_{rm}) = 2(1 - z_{rm})$ in Eq. (26).

$$\mathbb{R}_L = \left\{ \left[\frac{\hat{d}^2}{\hat{T}(\mathcal{M}_1 - \hbar_1 \mathcal{M}_2)} \right] + \left[\frac{R_{srm} \hat{C} (\mathcal{M}_1 - \hbar_1 \mathcal{M}_2)}{\hat{T} (\mathcal{M}_1 - \hbar_1 \mathcal{M}_2)} \right] + \left[\frac{1}{(\mathcal{M}_1 - \hbar_1 \mathcal{M}_2)} \right] \right\}$$

where,

$$\hbar_1 = \frac{\hat{\beta}^2 \hat{d}^3}{\hat{k}}; \mathcal{M}_1 = \frac{\hbar_3}{\hbar_2} + \frac{\hbar_4}{\hbar_2} + \frac{6-2D_R}{720}; \mathcal{M}_2 = \mathring{A}_3 + \frac{\hbar_5}{\hbar_2} + \frac{\hbar_6}{\hbar_2}; \hbar_7 = \frac{10-4D_R}{240 \hat{d} \hat{T} \hat{\beta}^2};$$

$$\mathring{A}_3 = \hbar_9 - \hbar_7 + \hbar_{11} + \frac{\hbar_{13}}{2} + \frac{\hat{d}^2}{6} - \frac{\hat{d}^2 D_{MR}}{12 \tau_m}; \hbar_8 = \mathcal{G}(\mathbb{C} + \mathcal{G} - 1)l; \hbar_9 = \frac{\mu(2-D_R)}{\hat{T} 12};$$

$$\mathring{A}_1 = \hbar_7 \hbar_8 + \hbar_9 \hbar_{10} + \hbar_{11} \hbar_{12} + \hbar_{13} \hbar_{14} + \hat{d}^2 (\hbar_{15} + \hbar_{16}); \hbar_{10} = \frac{\hbar_{16}}{\mathbb{C}};$$

$$\mathring{A}_2 = \hbar_8 \hbar_{16} + \hbar_{10} \hbar_{17} + \hbar_{12} \hbar_{18} + \hbar_{19} + \hbar_{20} - 2\hbar_{15} \tau \hat{d}^2 D_{MR};$$

$$\hbar_{11} = \frac{\hat{d}(3-2D_R)}{6 \hat{T}} + \frac{\hat{d}^2(1-D_R)}{2\hat{T}}; \hbar_{13} = \frac{\hat{d}^2(1-D_R)}{2\hat{T}};$$

$$\hbar_{16} = \frac{D_{MR} \mathcal{G}}{\tau_m 3} - \frac{D_{MR} (l - \mathcal{G} - 1) 2}{\tau_m \mathcal{G}^2}; \hbar_{18} = \mathcal{G}^2 \mathbb{C}; \hbar_{17} = \mathcal{G} \mathbb{C} (1 - \mathcal{G} - l);$$

$$\hbar_{21} = -1 + \frac{\mathcal{G}}{2} - \frac{\mathbb{C} - 1}{\mathcal{G}} + \frac{D_{MR}}{\tau_m}; \hbar_{16} = \frac{-D_{MR} \mathcal{G}}{\tau_m 3} - \frac{D_{MR} (\mathcal{G} + \mathbb{C} - 1) 2}{\tau_m \mathcal{G}^2};$$

$$\hbar_{20} = -1 + \mathcal{G} + \mathbb{C}; \hbar_{19} = \mathcal{G}(1 - \mathbb{C}); \hbar_{12} = \mathcal{G}(-\mathbb{C} + 1)l;$$

$$\hbar_{14} = \frac{1 - \mathbb{C}\mathcal{G} - \mathbb{C}}{\mathbb{C}}; \hbar_{15} = -1 - \frac{\mathcal{G}}{2} + \frac{l-1}{\mathcal{G}} + \frac{D_{MR}}{\tau_m};$$

6. Graphical Interpretations

The physical configuration of the problem of Darcy Brinkman Rayleigh Benard Two-Component (DBRBTC) Convection in a two-layered system has been investigated for linear, parabolic and inverted parabolic salinity gradients with the Dufour effect. To find the eigenvalue for dimensionless factors such as Darcy number (\mathcal{D}_a), viscosity (μ), Solutal Rayleigh number (\mathcal{R}_s), Dufour number for fluid

layer (\mathcal{D}_R), Dufour number for porous layer (\mathcal{D}_{MR}), variations in the Rayleigh numbers \mathbb{R}_L , \mathbb{R}_P and \mathbb{R}_I against the depth ratio (\hat{d}) for all three gradients for concentration are plotted. Now set $\mathcal{D}_a = 0.0001$, $\mu = 2$, $\mathcal{R}_s = 1000$, $\kappa = 2$, $\tau = 0.2$, $\tau_m = 0.75$, $\mathcal{D}_R = 5$, $\mathcal{D}_{RM} = 75$, $\hat{S} = 1$, $\hat{T} = 1$.

Figure 2, Figure 3 and Figure 4 show the difference in critical Rayleigh numbers \mathbb{R}_L , \mathbb{R}_P and \mathbb{R}_I versus depth ratio for different values of $\mathcal{D}_a = 0.0001$, $\mathcal{D}_a = 0.001$ and $\mathcal{D}_a = 0.01$ for LSP, PSP and ISP. The graph shows that \mathcal{D}_a has a destabilizing influence on DBRBTC convection because of \mathbb{R}_L , \mathbb{R}_P and \mathbb{R}_I de-escalate as the value of \mathcal{D}_a increases, permeability of the medium is improved for improved values of \mathcal{D}_a so the system is unstable for all the three salinity profiles.

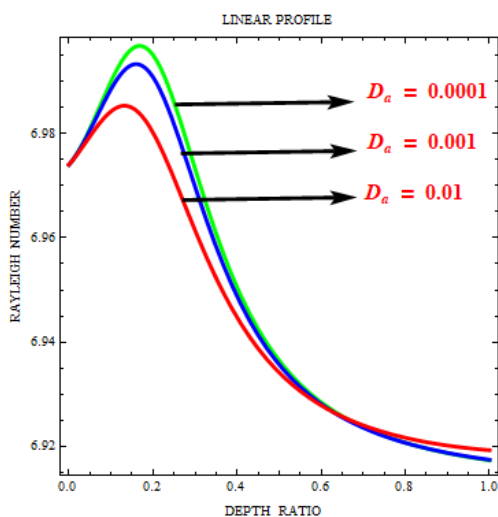


Fig. 2. Linear salinity profile for the effect of \mathcal{D}_a on Rayleigh Number \mathbb{R}

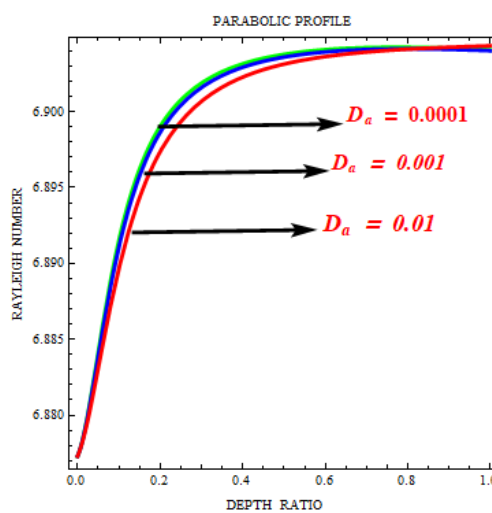


Fig. 3. Parabolic salinity profile for the effect of \mathcal{D}_a on Rayleigh Number \mathbb{R}

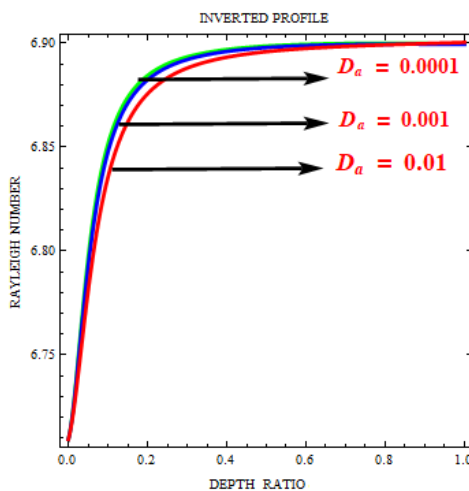


Fig. 4. Inverted parabolic salinity profile for the effect of \mathcal{D}_a on Rayleigh Number \mathbb{R}

Figure 5-Figure 7 show the difference in critical Rayleigh numbers \mathbb{R}_L , \mathbb{R}_P and \mathbb{R}_I versus depth ratio for different values of $\mathcal{D}_{MR} = 25, \mathcal{D}_{MR} = 50$ and $\mathcal{D}_{MR} = 75$ for LSP, PSP and ISP. The graph shows that the Dufour parameter for porous layer \mathcal{D}_{RM} has a stabilizing influence on DBRBTC convection because of $\mathbb{R}_L, \mathbb{R}_P$ and \mathbb{R}_I escalate as the values of \mathcal{D}_{MR} increases. Resistance of flow is increases for improved values of \mathcal{D}_{MR} so the system is stable for all the three salinity profiles. And also, the Dufour parameter for fluid layer \mathcal{D}_R plays a same role compared to Dufour parameter for porous layer \mathcal{D}_{MR} has shown in the Figure 8-Figure 10.

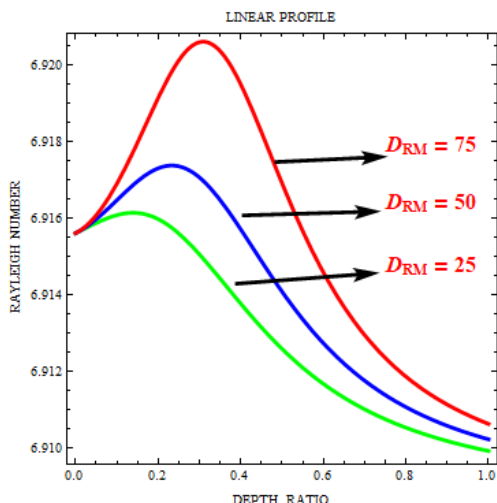


Fig. 5. Linear salinity profile for the effect of \mathcal{D}_{RM} on Rayleigh Number \mathbb{R}

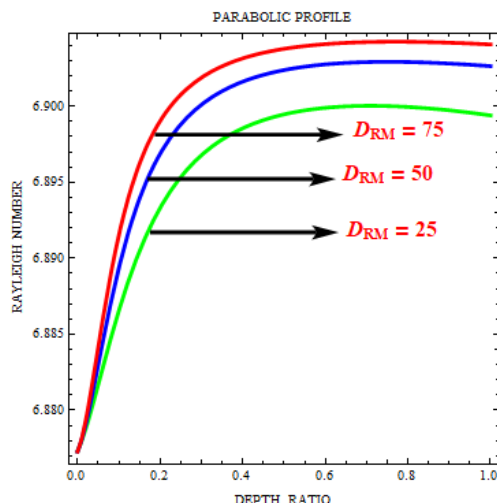


Fig. 6. Parabolic salinity profile for the effect of \mathcal{D}_{RM} on Rayleigh Number \mathbb{R}

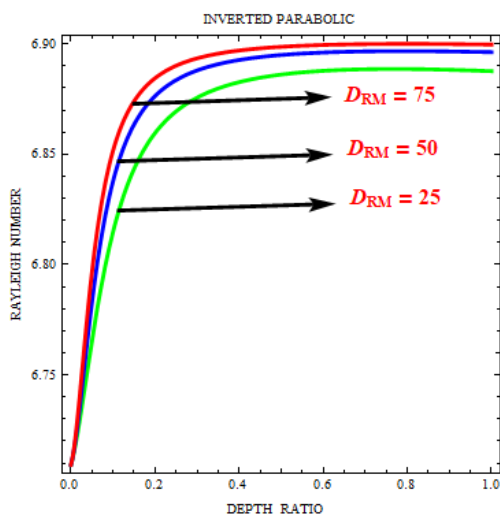


Fig. 7. Inverted parabolic salinity profile for the effect of \mathcal{D}_{RM} on Rayleigh Number \mathbb{R}

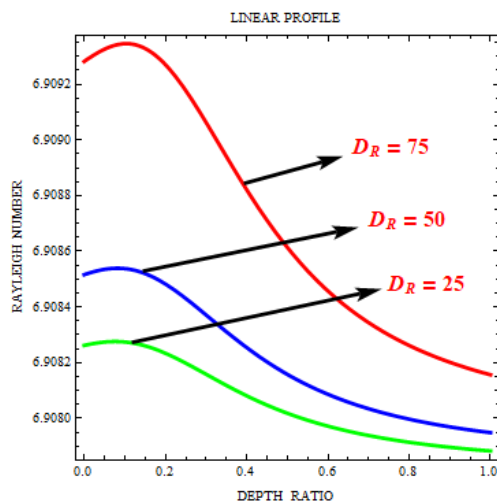


Fig. 8. Linear salinity profile for the effect of \mathcal{D}_R on Rayleigh Number \mathbb{R}

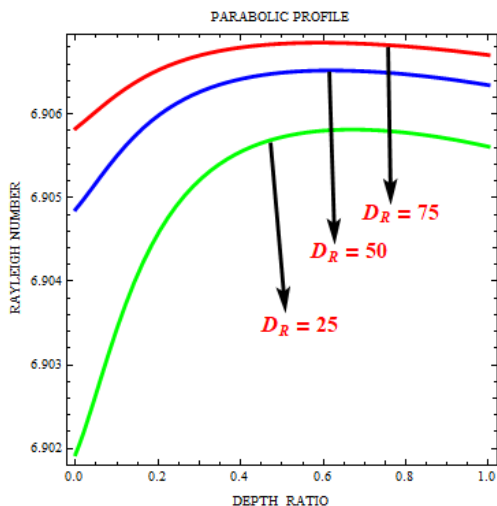


Fig. 9. Parabolic salinity profile for the effect of \mathcal{D}_R on Rayleigh Number \mathbb{R}

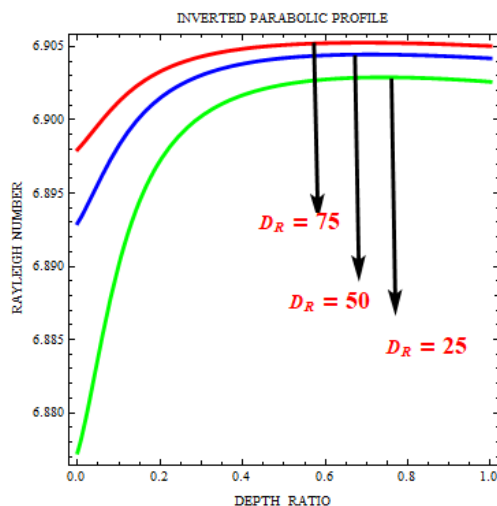


Fig. 10. Inverted parabolic salinity profile for the effect of \mathcal{D}_R on Rayleigh Number \mathbb{R}

Figure 11-Figure 13 show the difference in critical Rayleigh numbers \mathbb{R}_L , \mathbb{R}_P and \mathbb{R}_I versus depth ratio for different values of $\mu = 1, \mu = 2$ and $\mu = 3$ for LSP, PSP and ISP. The graph shows that μ has a destabilizing influence on DBRBTC convection because of $\mathbb{R}_L, \mathbb{R}_P$ and \mathbb{R}_I de-escalate as the values of μ increases, so the system is unstable for all the three salinity profiles.

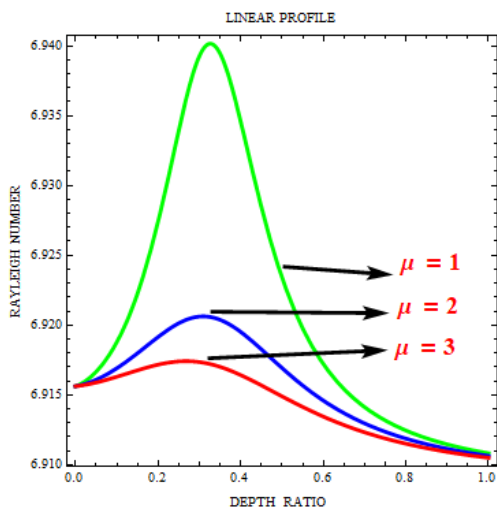


Fig. 11. Linear salinity profile for the effect of μ on Rayleigh Number \mathbb{R}

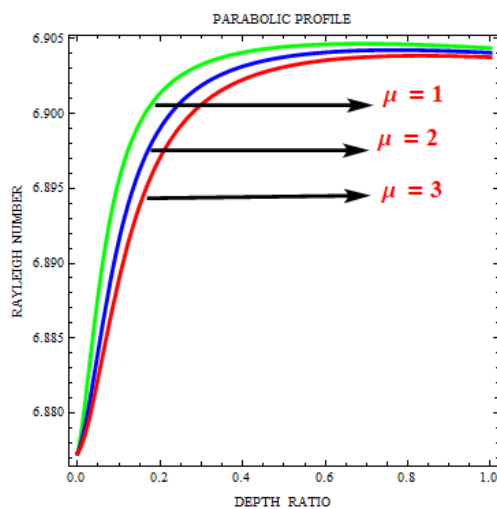


Fig. 12. Parabolic salinity profile for the effect of μ on Rayleigh Number \mathbb{R}

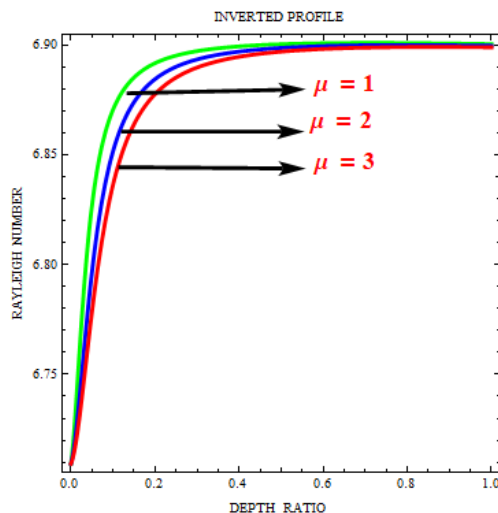


Fig. 13. Inverted parabolic salinity profile for the effect of μ on Rayleigh Number \mathbb{R}

Figure 14-Figure 16 show the difference in critical Rayleigh numbers \mathbb{R}_L , \mathbb{R}_P and \mathbb{R}_I versus depth ratio for different values for LSP, PSP and ISP. The graph shows that Solutal Rayleigh number (\mathcal{R}_S) has stabilizing influence on DBRBTC convection because of \mathbb{R}_L , \mathbb{R}_P and \mathbb{R}_I escalate as the values of \mathcal{R}_S increases so the system is stable for all the three salinity profiles.

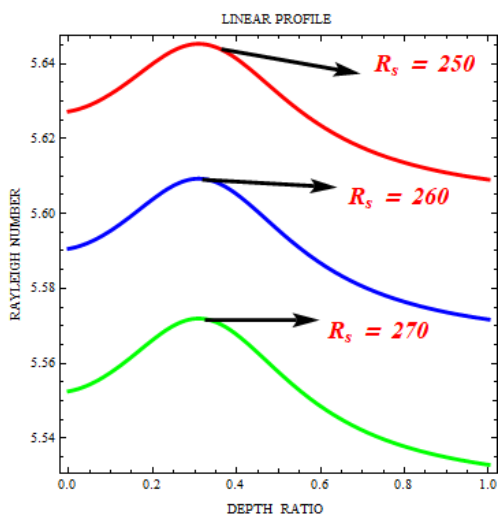


Fig. 14. Linear salinity profile for the effect of R_s on Rayleigh Number \mathbb{R}

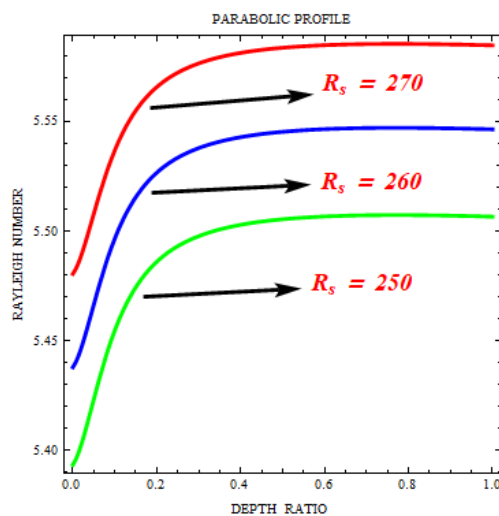


Fig. 15. Parabolic salinity profile for the effect of R_s on Rayleigh Number \mathbb{R}

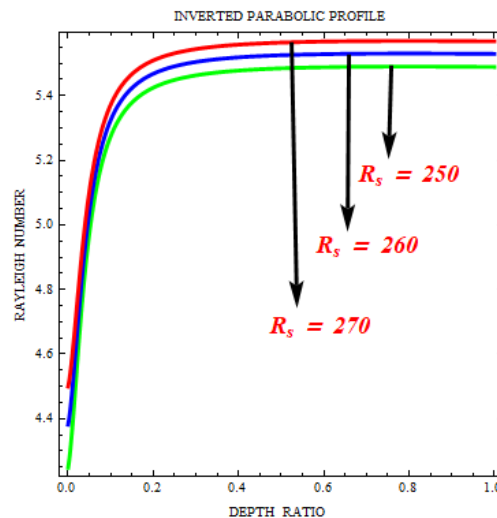


Fig. 16. Inverted parabolic salinity profile for the effect of R_s on Rayleigh Number \mathbb{R}

7. Conclusion

The effect of LSP, PSP and ISP on the onset of DBRBTC Convection in a two layer/Composite system along with Dufour effect has been explored. The expressions for the LSP, PSP and ISP Rayleigh numbers are found as functions of various dimensionless quantities and their influence on the stability of the system is depicted graphically. And the following findings are made from the study.

TCRB Convection in a Composite layer system with the Dufour effect is solved in closed form using the Regular Perturbation method and the following deductions are made from the study.

- i. Solute Rayleigh number (\mathcal{R}_s) is more effective for the least values of the depth ratio (\hat{d}) compared to all other physical parameters in all three salinity profiles.
- ii. The cross-diffusion effects like Dufour effects play a vital role in DBRBTC convection. The effect of Dufour parameters ($\mathcal{D}_R, \mathcal{D}_{MR}$) in both fluid and porous layers are stabilizing the composite system more effectively.
- iii. Both the viscosity ratio (μ) and Darcy number (\mathcal{D}_a) hasten the development of DBRBTC.

Acknowledgement

The first author R Sumithra expresses her heartfelt thanks to VGST, KSTEPS, Bengaluru, Karnataka, India, for sponsoring this investigation under K – FIST L2, Two years Research Project Scheme, of the Academic year 2020-21.

References

- [1] Altawallbeh, A. A. "Cross diffusion effect on linear and nonlinear double diffusive convection in a viscoelastic fluid saturated porous layer with internal heat source." *Fluids* 6, no. 5 (2021): 182. <https://doi.org/10.3390/fluids6050182>
- [2] Al-Mudhaf, Ali F., A. M. Rashad, Sameh E. Ahmed, Ali J. Chamkha, and S. M. M. El-Kabeir. "Soret and Dufour effects on unsteady double diffusive natural convection in porous trapezoidal enclosures." *International Journal of Mechanical Sciences* 140 (2018): 172-178. <https://doi.org/10.1016/j.ijmecsci.2018.02.049>
- [3] Aly, Abdelraheem M., Ehab Mahmoud Mohamed, Mohamed F. El-Amin, and Noura Alsedais. "Double-diffusive convection between two different phases in a porous infinite-shaped enclosure suspended by nano encapsulated phase change materials." *Case Studies in Thermal Engineering* 26 (2021): 101016. <https://doi.org/10.1016/j.csite.2021.101016>

- [4] Bandaru, Mallikarjuna, and R. Bhuvana Vijaya. "Effect of variable thermal conductivity on convective heat and mass transfer over a vertical plate in a rotating system with variable porosity regime." *Journal of Naval Architecture and Marine Engineering* 11, no. 1 (2014): 83-92. <https://doi.org/10.3329/jname.v11i1.16488>
- [5] Gbadeyan, J. A., T. L. Oyekunle, P. F. Fasogbon, and J. U. Abubakar. "Soret and Dufour effects on heat and mass transfer in chemically reacting MHD flow through a wavy channel." *Journal of Taibah University for Science* 12, no. 5 (2018): 631-651. <https://doi.org/10.1080/16583655.2018.1492221>
- [6] Hamrelaine, Salim, Fateh Mebarek-Oudina, and Mohamed Rafik Sari. "Analysis of MHD Jeffery Hamel flow with suction/injection by homotopy analysis method." *Journal of Advanced Research in Fluid Mechanics and Thermal Sciences* 58, no. 2 (2019): 173-186.
- [7] Tan, Jian Hong, Toru Yamada, Yutaka Asako, Lit Ken Tan, and Nor Azwadi Che Sidik. "Study of Self Diffusion of Nanoparticle Using Dissipative Particle Dynamics." *Journal of Advanced Research in Numerical Heat Transfer* 10, no. 1 (2022): 1-7.
- [8] Kotnurkar, Asha S., and Namrata Kallollikar. "Effect of Surface Roughness and Induced Magnetic Field on Electro-Osmosis Peristaltic Flow of Eyring Powell Nanofluid in a Tapered Asymmetric Channel." *Journal of Advanced Research in Numerical Heat Transfer* 10, no. 1 (2022): 20-37.
- [9] Murali, K., V. Kesavulu Naidu, and B. Venkatesh. "Solution of Darcy-Brinkman-Forchheimer equation for irregular flow channel by finite elements approach." In *Journal of Physics: Conference Series*, vol. 1172, no. 1, p. 012033. IOP Publishing, 2019. <https://doi.org/10.1088/1742-6596/1172/1/012033>
- [10] Malashetty, M. S., S. N. Gaikwad, and Mahantesh Swamy. "An analytical study of linear and non-linear double diffusive convection with Soret effect in couple stress liquids." *International Journal of Thermal Sciences* 45, no. 9 (2006): 897-907. <https://doi.org/10.1016/j.ijthermalsci.2005.12.005>
- [11] Nield, Donald A., and Adrian Bejan. *Convection in porous media*. Vol. 3. New York: springer, 2006.
- [12] Abidin, Nurul Hafizah Zainal, Nor Fadzillah Mohd Mokhtar, Izzati Khalidah Khalid, and Siti Nur Aisyah Azeman. "Oscillatory Mode of Darcy-Rayleigh Convection in a Viscoelastic Double Diffusive Binary Fluid Layer Saturated Anisotropic Porous Layer." *Journal of Advanced Research in Numerical Heat Transfer* 10, no. 1 (2022): 8-19.
- [13] Pal, Dulal, Bhuban Chandra Das, and Kuppalapalle Vajravelu. "Magneto-Soret-Dufour thermo-radiative double-diffusive convection heat and mass transfer of a micropolar fluid in a porous medium with Ohmic dissipation and variable thermal conductivity." *Propulsion and Power Research* 11, no. 1 (2022): 154-170. <https://doi.org/10.1016/j.jprr.2022.02.001>
- [14] Postelnicu, Adrian. "Influence of a magnetic field on heat and mass transfer by natural convection from vertical surfaces in porous media considering Soret and Dufour effects." *International Journal of Heat and Mass Transfer* 47, no. 6-7 (2004): 1467-1472. <https://doi.org/10.1016/j.ijheatmasstransfer.2003.09.017>
- [15] Rana, G. C., and R. C. Thakur. "Combined effect of suspended particles and rotation on double-diffusive convection in a viscoelastic fluid saturated by a Darcy-Brinkman porous medium." *The Journal of Computational Multiphase Flows* 5, no. 2 (2013): 101-113. <https://doi.org/10.1260/1757-482X.5.2.101>
- [16] Rosevear, Madelaine Gamble, Bishakhdatta Gayen, and Benjamin Keith Galton-Fenzi. "The role of double-diffusive convection in basal melting of Antarctic ice shelves." *Proceedings of the National Academy of Sciences* 118, no. 6 (2021): e2007541118. <https://doi.org/10.1073/pnas.2007541118>
- [17] Raizah, Zehba, and Abdelraheem M. Aly. "Double-diffusive convection of a rotating circular cylinder in a porous cavity suspended by nano-encapsulated phase change materials." *Case Studies in Thermal Engineering* 24 (2021): 100864. <https://doi.org/10.1016/j.csite.2021.100864>
- [18] Raizah, Zehba, and Abdelraheem M. Aly. "A rotating superellipse inside a hexagonalshaped cavity suspended by nano-encapsulated phase change materials based on the ISPH method." *International Journal of Numerical Methods for Heat & Fluid Flow* 32, no. 3 (2022): 956-977. <https://doi.org/10.1108/HFF-03-2021-0220>
- [19] Sumithra, R., N. Manjunatha, and B. Komala. "Effects of heat source/sink and non-uniform temperature gradients on non-Darcian-Bènard-magneto-Marangoni convection in an infinite horizontal composite layer." *International Journal of Applied Engineering Research* 15, no. 6 (2020): 600-608.
- [20] Sumithra, R., and N. Manjunatha. "Effects of Heat Source/Sink and non uniform temperature gradients on Darcian-Benard-Magneto-Marangoni convection in composite layer horizontally enclosed by adiabatic boundaries." *Malaya Journal of Matematik* 8, no. 2 (2020): 373-382. <https://doi.org/10.26637/MJM0802/0010>
- [21] Srinivas, S., A. Subramanyam Reddy, and T. R. Ramamohan. "A study on thermal-diffusion and diffusion-thermo effects in a two-dimensional viscous flow between slowly expanding or contracting walls with weak permeability." *International Journal of Heat and Mass Transfer* 55, no. 11-12 (2012): 3008-3020. <https://doi.org/10.1016/j.ijheatmasstransfer.2012.01.050>
- [22] Srinivasacharya, D., N. Srinivasacharyulu, and Ojjela Odelu. "Flow and heat transfer of couple stress fluid in a porous channel with expanding and contracting walls." *International Communications in Heat and Mass Transfer* 36, no. 2 (2009): 180-185. <https://doi.org/10.1016/j.icheatmasstransfer.2008.10.005>

- [23] Salleh, Hamidon, Amir Khalid, Syabillah Sulaiman, Bukhari Manshoor, Izzuddin Zaman, Shahrin Hisham Amirnordin, Amirul Asyraf, and Wahid Razzaly. "Effects of Fluid Flow Characteristics and Heat Transfer of Integrated Impingement Cooling Structure for Micro Gas Turbine." *CFD Letters* 12, no. 9 (2020): 104-115. <https://doi.org/10.37934/cfdl.12.9.104115>
- [24] Osalusi, Emmanuel, Jonathan Side, and Robert Harris. "Thermal-diffusion and diffusion-thermo effects on combined heat and mass transfer of a steady MHD convective and slip flow due to a rotating disk with viscous dissipation and Ohmic heating." *International Communications in Heat and Mass Transfer* 35, no. 8 (2008): 908-915. <https://doi.org/10.1016/j.icheatmasstransfer.2008.04.011>
- [25] Osalusi, Emmanuel, Jonathan Side, and Robert Harris. "The effects of Ohmic heating and viscous dissipation on unsteady MHD and slip flow over a porous rotating disk with variable properties in the presence of Hall and ion-slip currents." *International Communications in Heat and Mass Transfer* 34, no. 9-10 (2007): 1017-1029. <https://doi.org/10.1016/j.icheatmasstransfer.2007.05.009>